FINAL REPORT

Title: Ice Thickness Distribution

PI's: Norbert Untersteiner and Richard E. Moritz
Polar Science Center, Applied Physics Laboratory
University of Washington
1013 NE 40th Street, Seattle, WA 98105-6698
Telephone (206)-543-6613

Contract Number N00014-87-K-0635
Contract Start-End Dates 9-01-87 through 9-30-89

Summary

Prototype Upward Looking Sonar (ULS) instruments that monitor time series of ice draft from oceanographic moorings have been designed, built, tested and deployed in arctic waters. The measured time series recovered from these instruments reveal many geophysically significant, quantitative aspects of the sea ice draft distribution that have not been measured or documented previously. The utility of the basic concept, and the soundness of the ULS Mark-1 design are confirmed by the data. Tests in the laboratory and in the field suggest opportunities for modest design changes that would improve the performance of the ULS. Proposed further work includes implementation of design modifications, detailed analysis of the ULS time series, redeployment of the prototype units, and construction and deployment of three new ULS units.

Introduction and Background

The geophysical study of sea ice requires that it be described in terms of a number of state variables. Using the equations of dynamics and thermodyanmics these variables are combined to describe the behavior of the ice and its interaction with the adjacent media of atmosphere and ocean. Given the complexity of sea ice on geophysical scales, it is crucial that these state variables be chosen to describe the most important characteristics of the material, that they be suitable for mathematical formulation, and that they lend themselves to easy and accurate observation. Obvious first-choice state variables are *ice drift velocity* and *ice thickness*. For large scale model calculations to be meaningful, they must reproduce at least ice velocity and mean thickness (including zero, i.e. the ice edge) as functions of space and time. Together, these state variables must describe the overall ice balance of a region so that the total amounts of newly formed and melted ice and the ice transports may be calculated, on seasonal and interannual time scales, as they actually occur in the ice cover. It follows that, to assess and improve large scale sea ice models their output should be compared with observations of ice velocity and ice thickness.

It is an unfortunate coincidence that, of the geophysically most important state variables, only

velocity lends itself to accurate, long-term and economical observation (by satellite navigation of buoys and sequential images from synthetic aperture radar). The observation of ice thickness is, by comparison, difficult, lacking in spatial and temporal coverage, and expensive:

(1) Until the advent of nuclear submarines all thickness information was gathered (and some of it still is, e.g. Vinje and Finnekasa, 1986; Bourke and Paquette, 1989) by manually drilling or melting holes in the ice. What has been known for some time from these measurements is that the average winter ice thickness over most of the Arctic Basin is in the neighborhood of three meters. These data also serve as a basis for relating measurements of ice draft to ice thickness.

(2) Nuclear submarines travelling under the ice and recording ice draft by a sonar beam directed upward have gathered valuable information on the statistics of ice draft over long transects (e.g. Rothrock and Thorndike, 1980; Bourke and Garrett, 1987; Wadhams, 1983; 1990). Because of the nature of these submarine missions, their observations are not designed to give the spatial coverage of most scientific use, nor is their timing such that they can document trends of ice thickness over time. Many of the submarine data are not available for general scientific use, and detailed information on calibration, accuracy and resolution is often unavailable. Uncertainties in the absolute calibration of upward looking sonar profiles acquired from submarine cruises can limit their usefulness for resolving ice draft variability in the geophysically important range $h < 60\ cm$ (Bourke and Garrett, 1987).

(3) Passive microwave brightness temperatures measured by the satellite-borne ESMR and SMMR instruments are theoretically capable of distinguishing first-year from multi-year ice (e.g. Parkinson, et al., 1987). While the relationship between ice age and thickness is not unique, age is nevertheless a first approximation to thickness. In principle, one could assign average thicknesses to first-year and multi-year ice, extract the relative abundances of these ice types from time series of the satellite data, and arrive at an estimate of the annual ice production over a region. However, there are insufficient ice thickness data with which to calibrate the average thickness to be assigned to the ice types. Furthermore, there are significant uncertainties about the relationship between ice type abundance and passive microwave measurements. This situation is but one example of the intrinsic difficulty of obtaining ground truth for calibrating ice type algorithms. Passive microwave pixels are 20 kilometers square and larger, and it is extremely difficult and laborious to determine from measurements on the ice surface how much first-year, multi-year, new and deformed ice such a pixel actually contains.

(4) Even if the *average* ice thickness could be monitored from space at all locations and times, it would not provide an adequate basis for scientific progress and the development of better predictive models. Both the thermodynamic and dynamic behavior of the pack depend on the *ice thickness distribution G(h)*. $G(h)$ is the fractional area covered by ice thinner than h. Although a theory for the time and space variations of $G(h)$ has been available for many years (Thorndike, et al.,

1975), we have only the most rudimentary ice thickness data with which to determine the specific functions and coefficients that would make the theory applicable to geophysical problems (Thorndike, 1980; Rothrock, 1986).

In summary, a concerted effort is needed to obtain accurate, time series data on the ice draft distribution, at a number of locations in the polar seas. This report describes research activities carried out over the period 9/1/87-9/30/89, that initiated the systematic acquisition of time series data on ice draft. The main thrust of the project is the design, construction, testing and application of an upward looking sonar instrument that accurately monitors $G(h)$ from oceanographic moorings. Following a brief restatement of the project objectives, individual sections of the report describe our efforts in each of these areas.

Objectives

(1) Design a stationary, moored upward looking sonar (ULS) for measuring the draft of sea ice passing over oceanographic moorings.

(2) Calibrate and test the ULS components in the laboratory and in the nearby waters of Lake Washington and Puget Sound.

(3) Build two ULS units, deploy them in ice covered polar waters, and recover them after one year of operation.

(4) Analyze the data stored in the two ULS units to assess instrument performance, and to determine the statistics and principal features of the ice draft time series. Compare the ULS measurements with ice charts, remote sensing imagery, and related weather data, and interpret the average and time variable properties of the ice draft distributions sampled by the ULS.

(5) Based on the results, identify needed modifications to the prototype ULS design.

(6) Redeploy the ULS units on moorings of opportunity.

Technical Approach

Measurement and Operating Requirements

The basic variable of interest is ice draft h, defined at any point on the ocean's surface as the distance measured along the local vertical from the bottom of the sea ice to local sea level. Because the physical properties of the pack are sensitive to the area of thin ice and open water, it is desirable to resolve small differences in ice draft for thin ice. A reasonable goal for individual measurements of ice draft is to keep typical errors smaller than about 10 centimeters. Our approach to measuring h is to measure simultaneously two quantities: (a) the distance h_1 from the ULS to sea level; and (b) the distance h_2 from the ULS to the underside of the sea ice (Figure 1). The ice draft is the difference

$$h = h_1 - h_2 \ . \tag{1}$$

h_1 is derived from the hydrostatic pressure at the ULS, measured by a precise barometer. h_2 is derived from the elapsed time for an acoustic pulse to travel from the ULS to the bottom of the ice and return, measured with a high frequency sonar and precision clock. Time series statistics are needed to represent the mean ice draft and ice draft distribution for a finite region of ice passing over the mooring. It follows that the ULS must acquire many samples of the ice in each such region. On the other hand, the statistical significance of the sample is maximized (subject to the constraints imposed by memory size and battery life) if successive measurements are statistically independent. In typical ice conditions, these considerations dictate an optimal sampling interval on the order of five minutes. Due to the difficulty and expense of field work in ice-covered waters, it is desirable that the ULS operate autonomously for at least one year. Year-long operation has the advantage that both deployment and recovery can be carried out during those seasons when the ice covered sea is most accessible. That is, late summer for ships, and early spring for aircraft that land on the ice. To facilitate transport, deployment, and recovery, the ULS must be small and lightweight. It is also important to design a ULS of low to moderate cost, so that it becomes a typical and useful article in the polar oceanographer's equipment. The ULS must function successfully at the top of mooring lines from tens to thousands of meters long, in variable currents with speeds up to .5 m/s, and in rough ice with keels up to 50 m deep. The ULS controller program must operate for time periods up to one hour (during deployment) in air temperatures as low as $-30^o\ C$, and for extended periods (one year) at $-2^o\ C$. The ULS must be sufficiently rugged to survive typical mooring operations in ice-covered waters. Finally, data storage and security must be provided in the event of exhaustion of the power supply or shutdown of the ULS controller program.

To determine h_1 it is necessary to measure hydrostatic pressure p at the ULS and at sea level p_a . These quantities are related to the distance h_1 by the hydrostatic equation

$$h_1 = \frac{p - p_a}{\rho_w\ g} \ . \tag{2}$$

A typical value for h_1 is 60 m, as dictated by the joint constraints of keel avoidance, sonar range and spatial resolution, and this value is used to calculate approximate error tolerances. Errors in each of the quantities appearing in equation (2) contribute to errors in h_1 . The error contributed by inaccuarcies in any single quantity is no larger than 10 cm if that quantity is known with a relative precision of 10 $cm/60\ m$ = one part in six hundred. This relative precision translates into absolute precision of approximately 800 Pascals for the pressures p and p_a , about .015 m/s^2 for gravity g, and about 1.708 kg/m^3 for the density of seawater ρ_w . The width of the sonar beam is characterized by y, the angular deviation (measured in degrees) from the acoustic axis at which the beam response is 3 dB less than its maximum value on the axis. If the reflecting surface (ice) is flat, the acoustic energy within this beam impinges on a circular area F called the "footprint". The logic and gain in the ULS receiver may be set so that the reflection of the acoustic pulse from which h_2 is derived occurs within this footprint with high probability. Of course the ice is not flat, and the draft h varies with position over the area F. ULS Mark-1 records the first received echo that exceeds a fixed threshold, corresponding essentially to the deepest ice within F and the smallest distance h_2 .

This procedure leads to bias in the ice draft statistics, but the bias is no larger than the range of h over the area F. Rothrock and Thorndike (1980, their Figure 8) present the spatial autocovariance of ice draft estimated from a submarine sonar profile in the Beaufort Sea. Interpolating from their plot, the ice draft typically changes by $\pm$ 30 *cm* over a horizontal distance of $r_o \approx 3\ m$. A footprint of diameter $2r_o = 3m$ corresponds to a beamwidth $y \approx 1.5^o$ at a distance $h_2 = 60\ m$. Johnsen (1989) estimates the bias based on high resolution, 2-dimensional maps of ice draft, obtained with a manually operated scanning sonar deployed through a hole in the ice. Assuming the ULS records the return from the nearest ice in the footprint, he finds that an instrument with beamwidth $y \approx 5^o$ deployed at depth $h_2 = 60\ m$ would have a bias of approximately +25 *cm*, and that bias is roughly proportional to y for small values of y. The estimate is based on scanning 44 icefloes including multiyear and first year ice. These results suggest that a beamwidth of 2^o may be adequate to keep the bias at or below 10 *cm*. For many applications of ULS data, such as estimating heat fluxes and opening, one needs greater measurement accuracy for thin ice than for thick ice. The *conditional statistics of ice draft, given that* $h < h_o$, differ in general from the unconditional statistics (cf. Colony, 1987). In particular, if the conditional variance of the spatial increment $h(\mathbf{x} + \mathbf{l}) - h(\mathbf{x})$ of ice draft, given $h(\mathbf{x}) < h_o$, is smaller than the overall variance of increments, at lags $|\mathbf{l}|$ on the order of 3 meters, then a ULS with a given beamwidth will have smaller errors in thin ice. Further analysis of this issue is underway, using existing submarine sonar profiles and the time series from the Chukchi ULS. In any event, bias is reduced by narrowing the beamwidth y, which is related to the footprint radius and the range according to

$$h_2\, y = r_o \quad . \tag{3}$$

The distance h_2 is estimated by measuring the time τ for the acoustic pulse to make a round trip between the ULS and the bottom of the ice:

$$h_2 = \frac{1}{2}\, \bar{c}\tau \tag{4}$$

where $\bar{c}$ is the average speed of sound in the seawater between the ULS and the ice. However, equation (4) holds only for a vertically directed acoustic pulse. If the pulse propagates at some angle ζ measured from the local vertical, then equation (4) overestimates h_2 by an amount $h_2\,(\sec(\zeta) - 1)$. With $h_2 = 60\ m$, the overestimate is 10 *cm* when $\zeta = 3.3^o$. In vertical orientation, $\bar{c}$ and τ must also be known to better than 1 part in 600 to achieve 10 *cm* accuracy for h_2 . These constraints yield maximum allowable errors of 2.4 *m/s* for $\bar{c}$ and 0.14 milliseconds for τ. Table 1 sets out the error limits that guided the engineering of the prototype ULS.

TABLE 1: ULS Performance Specifications

PARAMETER	SYMBOL	TOLERANCE
Air Pressure	p_a	800 Pa
Water Pressure	p	800 Pa
Gravity	g	.015 ms^{-2}
Density	ρ_w	1.7 $kg\ m^{-3}$
Beam Width	y	2^o
Zenith Angle	ζ	3^o
Sound Speed	$\bar{c}$	2.4 ms^{-1}
Travel Time	τ	$0.14 \times 10^{-3}\ s$
Sampling Interval		5 min
Operating Interval		1 year
Min Operating Temperature		$-2^o\ C$
Max Lens Temperature		$+35^o\ C$
Maximum Keel Draft		50 m
Max Current Speed		0.5 ms^{-1}

Results

Basic ULS Design

The prototype ULS (Mark-1) was designed to meet the criteria and operating constraints discussed in the previous section. The goal of an easily moored, lightweight, compact unit is realized by housing the ULS on a spherical 17-inch diameter glass oceanographic float (Figure 2). The sonar is mounted at the top of the float, the circuit boards and barometer are mounted inside the float, and the power pack is mounted on the bottom of the float. A standard plastic hard hat bolts over the sphere, with holes at top and bottom through which the sonar and power pack protrude. Metal guards protect the sonar and power pack. The power pack guard and the eyebolts that secure the hard hat provide points of attachment for mooring line. The ambient pressure is measured by a Paroscientific Digiquartz precision barometer, mounted on the inside of the glass sphere and ported to the seawater. The acoustic signal is generated by a 307 kHz transducer mounted on a gimbal and housed inside a plastic hemispherical lens filled with fluid. Slow changes in the fluid volume, due to the ambient temperature and pressure of the seawater, are compensated by a flexible plastic tube connected to the lens reservoir. The sound speed of the fluid and the radius and focal plane of the lens are chosen such that the acoustic pulse focuses into a narrow beam as it passes between the lens and seawater at the freezing point. The gimbal is weighted so that the transducer element aims vertically, independent of the tilt of the glass float. The power pack and the lens are connected to the electronics boards via wires that enter the sphere through sealed penetrators. The electronics boards are mounted on suction cups bonded to the glass sphere. The lower board controls the clock cycle and measurement operations of the ULS. The upper board contains 32 EPROM chips, providing a 1 Mb memory for data storage. The controller board supports a serial port, wired through a sealed penetrator to an external 4-pin connector. A small green light, mounted to the inside of the glass sphere facing out, indicates the operating status of the ULS.

The system logic is very simple. At a regular time interval (nominally 5 minutes), the output of the barometer is sampled by counting the number of system clock oscillations (frequency 307 kHz) during which the barometer oscillator executes 7000 cycles. This count is recorded as 4 bytes in the EPROM. During data reduction, the counts are converted to the period of the barometer oscillator. The calibration coefficients provided by Paroscientific are then used to find the pressure p as a function of the measured period. The calibration coefficients depend on temperature, and this effect is included in the calculation, using an assumed temperature representative of seawater beneath ice. Over the range of temperatures typically encountered in the upper 100 meters of ice-covered waters the variation of barometer coefficients is negligible. Each barometer measurement is accompanied by a sonar measurement, acquired as follows. A pulse of frequency 307 kHz, width 1 millisecond and rms amplitude 15 Volts excites the acoustic transducer. Simultaneously the microprocessor begins to count the oscillations in the system clock. The pulse propagates through the lens fluid, focuses at the lens-water interface, then propagates upward in a narrow beam. 7 milliseconds elapse before the ULS processor begins to listen for an echo from the ice. At typical sound speeds, this time corresponds to a propagation path of 10 m and to targets at a distance of 5 m. A fixed gain of 60 dB is applied to the voltage output of the transducer. When the voltage exceeds a pre-determined threshold of 2.4 Volts, the count is terminated, and the number of clock cycles is written as 4 bytes in the EPROM. The counts are converted directly to time τ, including adjustments for the portion of the propagation path inside the lens, and for software and detector delay times. The system logic for the prototype ULS instruments was chosen chiefly for its simplicity. Its usefulness depends on two factors: (1) At the maximum design range, the echo from the underside of sea ice must be sufficient to produce a measured voltage that exceeds the detection threshold; (2) At the minimum listening range (5 meters) the strongest possible false target must produce a measured voltage that does not exceed the threshold. In other words, sea ice at long range must present a significantly stronger target than any other oceanographic phenomena in the beam path, even at shorter range.

Strength of the Sonar Return

The acoustic pressure amplitude P, measured on the acoustic axis at 1 meter distance from the trasnducer, characterizes the transmitted and received signals near the ULS. During transmission (at time $\tau = 0$), the relevant parameter is the source level $SL = 20\log(P_t)$, measured in $dB\ re\ 1\mu Pa$. The corresponding parameter during reception (at time τ) is the received level $RL = 20\log(P_r)$. The difference $SL - RL$ depends on the acoustic environment within a hemisphere of radius $\bar{c}\tau/2$ centered on the ULS, and on the sonar beamwidth y. Let ε_R be the voltage output of the ULS receiver generated by a unit sound pressure amplitude $P_r = 1\ \mu Pa$, incident at one meter distance. The receive sensitivity of the system is $RCS = 20\log(\varepsilon_r)$, measured in $dB\ re\ 1V/\mu Pa$. For typical sonar receivers, RCS thus defined is negative. A fixed gain G is applied to the voltage output to produce the measured voltage level $MVL = RL + RCS + G$, that is monitored by the detection trigger. The detection trigger activates when the measured voltage increases to over 2.4 $Volts$, corresponding to a detection threshold $DT = 20\log(2.4) = 7.6\ dB\ re\ 1V$. Therefore, sea ice is *just* recorded by the ULS when it produces a received level such that $MVL = DT$, or

$RL_d = DT - RCS - G$. RL_d is the minimum received level that activates the detection trigger.

The difference $RL - SL$ may be related to the acoustic environment and the beamwidth using the sonar equations (eg. Urick, 1975). Essentially, the sonar equation is a statement of energy conservation applied to a pulse of sound as it executes a round trip from 1 meter outside the ULS to a target and return. A simple model for this process accounts for the dissipation of energy (propagation loss) between the ULS and the ice, the spreading with distance of the acoustic beam, and the reflection or backscattering of the pulse by the undersurface of the ice. If the ice is level (normal incidence), then the model takes the following forms for pure reflection:

$$RL = SL - 2\alpha h_2 - 20\log(2h_2) + 20\log(R_e) \tag{5}$$

and for pure scattering:

$$RL = SL - 2\alpha h_2 - 40\log(h_2) + 10\log(\psi h_2^2) + S_s \tag{6}$$

where α is the seawater absorption parameter for sound at frequency $\nu = 307\ kHz$, R_e is the effective normal incidence reflection coefficient for sea ice, ψ is the solid angle (steradians) subtended by the equivalent uniform-intensity beam pattern, and S_s is the scattering strength of the undersurface of sea ice. The source level for the Mark-1 ULS is 204 $dB\ re\ 1\mu Pa$. The beamwidth is approximately $y = 1.5^o$ (Figure 3). Experimental determinations yield $\alpha = .0645\ dB/m$ at temperature $T = -1.5^o\ C$, salinity $S = 30\ ^o/oo$, and frequency $\nu = 300\ kHz$ (Francois and Garrison, 1982). Measurements of the reflectivity of level sea ice suggest that $R_e \approx .03$ (Figure 4). Measurements of scattering strength of level sea ice reported by Francois (personal communication, 1991) fit the relationship $S_s = -72 + 25\ \log(\nu) + 15\ \log(\sin(\theta_g))$ where S_s is measured in $dB\ re\ 1\mu Pa$, ν in kHz and θ_g is the grazing angle between the sonar beam and the scattering surface. Urick (1975, p. 217) provides the formula $10\log(\psi) = 20\ \log(y) - 31.6$ that relates the beamwidth y in degrees to the equivalent beam solid angle ψ in steradians. Equipped with these numbers, and setting $\theta_g = \pi/2$ for normal incidence, we may estimate the variation of received level RL with distance h_2, for each of equations (5) and (6). The results are plotted in Figure 5. The agreement between the two curves is remarkable because they are based on independent measurements using different techniques. The minimum received level RL_d appears on this plot as a horizontal line, based on the parameters $RCS = -165\ dB$ and $G = 60\ dB$. Vertical lines denote the depths of the Chukchi ULS and the Scoresby ULS, in their 1988-89 deployments. According to the figure, 60 dB gain is sufficient for the ULS to "see" level ice in clear water at distances in excess of 100 meters.

Obviously, much sea ice is not level. When the undersurface of the ice above the ULS has a significant slope, the scattering model must be modified to account for oblique angles of incidence, and the simultaneous arrival at the ULS of sound scattered by ice at different distances, corresponding to the leading and trailing portions of the pulse. A model more appropriate for sloping ice is:

$$RL = SL - 2\alpha h_2 - 40\log(h_2) + S_s + 10\log(\psi h_2^2) + 20\log(\bar{c}\tau_p/(2h_2\cos\theta_g)) \tag{7}$$

where τ_p is the pulse length. Curves corresponding to $\theta_g = 10^o$ - 70^o are plotted on Figure 6. The reduction in received level due to various grazing angles is significant. One would expect a ULS with the indicated minimum receive level $RL_d = 112.6\ dB$ to fail to record ice drafts with grazing angles smaller than approximately 70 degrees at 60 meters distance.

Biota, such as fish, seals and plankton, sharp pycnocline layers, and bubbles that accompany breaking surface waves can in some circumstances be recorded as false targets by the ULS in arctic waters. Wave-generated bubbles are strong sonar scatterers that occur when open water is above the ULS, together with sufficient wind speed and fetch. However, the presence of such a bubble layer can be inferred by careful inspection of the ULS time series (cf. Data Report), and the implication for ice draft is simple: the ice draft is zero.

Significant acoustic scattering from biota concentrated in layers has been noted by Hunkins (1965), Feldman et al. (1973), and Garrison et al. (1985) during the summer and fall seasons. Garrison et al. (1987) found no significant scattering by such layers during a set of measurements in spring in the Beaufort Sea. It seems likely that the occurrence of such layers is controlled ultimately by the availability of light for photosynthesis, and therefore by the surface insolation and the ice cover. The occurrence of biota in thin layers may be related to a pycnocline or mixed layer base. The volume reverberation S_v (measured in $dB\ re\ m^{-3}$) produces a received level

$$RL = SL - 2\alpha h_2 - 40\log(h_2) + S_v + 10\log\left[\frac{\bar{c}\tau_p}{2}\right] + 10\log(\psi h_2^2). \qquad (8)$$

Francois (personal communication, 1991) reports a maximum value $S_{vmax} = -45\ dB$ measured in the Chukchi Sea during the peak of the plankton bloom. During other times of year S_v is considerably smaller. Equation (8) is plotted on Figure 7, which shows that peak reverberation levels can produce a received level in excess of RL_d, but only at distances smaller than about 3 meters. Typical reverberation levels are unlikely to trigger the ULS.

The normal-incidence coefficient of reflection from a pycnocline step may be estimated as

$$R_e = \frac{\rho_1 c_1 - \rho_2 c_2}{\rho_1 c_1 + \rho_2 c_2} \approx \frac{\Delta[\rho c]}{2\bar{\rho}\bar{c}} \qquad (5)$$

where $\bar{\rho} \approx 1026\ kg\ m^{-3}$ and $\bar{c} \approx 1440\ ms^{-1}$ are values typical of upper Arctic Ocean waters with temperature $T = -1.5^o\ C$ and salinity $S = 32^o/oo$. In the Arctic Ocean, such steps occur with fresher water above saltier water, because salinity controls the density stratification. The fresher water may be warmer or cooler than the underlying water. The former condition may occur at the seasonal pycnocline during the melt season, and the latter at the base of the mixed layer in winter. The reflection coefficient for temperature-salinity steps $(\Delta T, \Delta S) = (+1^o\ C, 0)$, $(0, -1^o/oo)$, $(+1^o\ C, -1^o/oo)$, $(-0.5^o\ C, -1^o/oo)$ are $R_e =$ (.003), (.002), (.002) and (.003) respectively. The received level corresponding to $R_e = .003$ is plotted on Figure 7, as computed from equation (5). If a step as large as $\Delta T = 1^o\ C$ actually occurs in the water column, it could cause a reflection sufficient to trigger the ULS at distances up to 35 meters. Furthermore, a step of this magnitude cannot be distinguished from ice at grazing angles greater than about 35^o on the basis of received level alone (Figures 6 and 7).

The received levels cited above are viewed as rough estimates that guided the choice of a gain setting $G = 60\ dB$ in the Mark-1 ULS. According to these estimates the most important factor in choosing a gain level is the effect of a sloping undersurface on the target strength of sea ice. The ULS should record the draft of all but the most steeply sloping ice at the nominal design range of 50 meters. Volume reverberation should never trigger the Mark-1 ULS but anomalously strong steps $\approx 1^{o}\ C$ in temperature structure constitute false targets at distances up to 35 meters.

The ULS Mark-1 was deployed in the Chukchi Sea at a depth of 44 meters (see Data Report). The data record for this instrument is complete. Over one year, the only instances where it failed to record a signal from the ice or open water surface occurred when a false target layer intervened. The ice conditions included young, first year, multiyear and ridged ice, and obvious cases of active ice growth and melt. Therefore, the 60 dB gain appears sufficient for the ULS Mark-1 to measure the draft of all types of ice at 44 meters distance. The false targets seen by the Chukchi ULS tend to occur in a thin layer approximately 17 meters above the instrument. The occurrence of these targets varies diurnally and with the amount of open water, suggesting control by light availability. Our tentative conclusion is that these targets are fish or large zooplankters, concentrated in a layer (possibly a pycnocline) where food is abundant. The ULS Mark-2 deployed in the Greenland Sea off Scoresbysund operated at a depth of 65 meters. This instrument recorded nearly 100% of the surface reflections during the first few weeks of operation, when open water occurred overhead. As soon as sea ice appeared, the number of "no echo" readings in the memory increased to the order of 50%, with large variations over week-long periods. It would appear that 60 dB is insufficient gain for the ULS Mark-1 at a distance of 65 meters. It should be noted that the seawater bubble formed in the lens by leakage was larger in the Scoresby ULS than in the Chukchi ULS. De-focusing due to the lens bubble would decrease the received level from all targets, but the magnitude of the effect is unknown. In light of the approximate calculations above, it seems plausible that the Scoresby ULS recorded most of the level ice, but only a much-reduced random sample of deformed ice with a sloping undersurface. This hypothesis is under further investigation, based on the Scoresby ULS time series (Data Report in preparation).

On deep water moorings, it is difficult to predict precisely the depth of the uppermost float, i.e. the ULS. Therefore, it is highly desirable to extend the range of ULS-1 to, say, 100 meters. In view of the potential significance of false targets, simply increasing the gain does not seem to be acceptable. New research efforts on ULS Mark-2 will approach the problem by developing two new features: (1) The ULS will set its "listening window" based on the barometer reading, so that it listens only for echos returning from distances in the range (approximate) 20 meters below sea level to 3 meters above sea level; (2) A stepwise time-variable gain (TVG) will increase G over time after the pulse is transmitted. Feature 1 eliminates the possibility of recording false targets unless they occur within 20 meters of the ice surface. Feature 2 is designed to assure sufficient gain for a 100 meter range, without increasing false target receptions when the ULS is closer to sea level.

In the prototype ULS, the basic sampling interval is programmable by the user in the range 2 seconds to 1 hour. The detection threshold, output gain and pulse amplitude are hard-wired.

The pulse length is not user-programmable, but it programmed into the ULS operating system.

Test Results at U.W.

Objectives (1)-(2) were accomplished in the first year of the project, as described in the previous Research Summary (appendix 1). In response to a request by the Norwegian NorskPolarinstitutt (NPI), two additional ULS units were built and sold at cost. The four prototype units are designated APL-ULS1, APL-ULS2, NPI-ULS1 and NPI-ULS2.

Field Deployments and Results

The deployment locations for the four prototype ULS units are shown on Figure 8. APL-ULS1 was deployed helicopter, with the aid of NOAA personnel, in the Chukchi Sea at latitude 71^{o} $36^{'}$ *N* longitude 158^{o} $43^{'}$ *W* on 15 April, 1988. The water depth was 55 meters. This unit was recovered by NOAA personnel using a helicopter, on 4/15/89. The ULS was completely functional on recovery, and yielded a full year's data from both acoustic and pressure sensors at five minute intervals. A data report is attached (appendix 2). Inspection of these data indicate that the unit succesfully monitored time series of ice draft. The data support the claim that the ULS unit can provide reliable monitoring data on the ice thickness distribution, and thereby fill the most serious data gap in our knowledge of surface processes on the polar oceans. Further analysis of these data is underway.

APL-ULS2 was deployed from the RV *Saemundson,* with the aid of personnel from the Marine Research Institute in Reykavik, in the Greenland Sea at latitude 70^{o} $59^{'}$ *N* longitude 19^{o} $0^{'}$ *W* on 10 September, 1988. The water depth was 822 meters. This unit was recovered in September, 1989. Inspection of the data reveals gaps in the record, but the unit made geophysically useful measurements of ice draft from September, 1988 to February, 1989, at which time the microprocessor program failed. On recovery, the unit began to operate normally again, and the system clock reported the correct time and date. The causes of the data gaps and program shutdown are under investigation.

NPI-ULS1, purchased by the Norsk Polarinstitutt, was deployed from the RV *Endeavor,* with the aid of personnel from the Woods Hole Oceanographic Institution, in Fram Strait at latitude 79^{o} $26^{'}$ *N* longitude 6^{o} $48^{'}$ *E* on 24 August, 1988, at the top of the RTEAM mooring. The water depth was 1270 meters. NPI-ULS1 was recovered on 9 October, 1988. The unit was damaged during recovery or shipment, while still powered on, resulting in the loss of most of the measurements. However, satellite data show that sea ice was never present over the RTEAM mooring, so there was no loss of ice draft information. Moreover, it was determined from the undamaged portion of the memory that the unit was functioning more than 1 week after deployment. The sea surface position measurements from the acoustic and pressure sensors tracked one another through a tidal cycle. There is no evidence to indicate that NPI-ULS1 would not have successfully measured ice draft if it were powered off immediately after recovery. The unit was refurbished at APL and shipped to Svalbard for redployment by NPI.

NPI-ULS2 was deployed from the RV *Polarstern,* in the Greenland Sea at latitude $78^o\ 27'\ N$ longitude $4^o\ 1'\ W$ on 29 June, 1988. The water depth was 1800 meters. Unfortunately, this unit was lost at sea with the upper portion of the mooring during recovery operations.

Performance Evaluation and Design Modifications

Although the basic ULS design is sound, deployment of the prototype units revealed several opportunites for improvement:

(1) Each unit exhibited a small water bubble inside the acoustic lens after several months in the water. The effect of such a bubble is a slight defocusing of the lens, so it is desirable to eliminate the leakage. The leakage is attributed to the pressure equalization hose and the fitting where this hose connects to the lens. It is proposed to incorporate a small bellows into the bottom of the lens housing, thereby eliminating both the pressure hose and the fitting.

(2) Laboratory cold box tests show that the ULS microprocessor can suffer read/write errors, and may even hang or shut down with prolonged exposure to temperatures below $-10^o\ C$. It is proposed to incorporate multiple read/write checks and a fail-safe wakeup circuit into the microprocessor design, to guard against these modes of failure.

(3) It would have been useful to know the temperature of the ULS, and thus the surrounding water mass, to help interpret the causes of time changes in the calculated ice draft when we believe open water is overhead. Are these changes caused by variations in sound speed and density? Recording the temperature would also aid in the diagnosis of any cold-related system failures. It is proposed to monitor the temperature signal of the Paros pressure gauge, and to record temperature approximately four times per day.

(4) APL-ULS2 failed to record acoustic returns in a significant number of samples when ice was overhead. We believe this failure is due to insufficient gain applied to the signal. This unit was moored approximately 70 meters below the ice. However, greater gain increases the likliehood of false target reflections from biota and other phenomena near the ULS. An adjustable gain and modified logic are proposed to improve performance in this area.

(5) Our confidence in instrument performance, and the interpretation of the statistics of ice draft sampled at 5 minute intervals would be enhanced by high-resolution profiles of limited duration, that resolve a sample of under-ice topography approximately once per day. It is proposed modify the software to permit programmable acquisition of high resolution profiles at regular intervals interspersed with the normal, lower resolution sampling.

(6) The use of lithium batteries creates problems in shipping and handling, and may constitute a health hazard under certain circumstances. It is proposed to change the power supply to high performance alkaline or other, safer cells, and to house the battery pack inside the glass sphere, making the ULS easier and safer to handle and transport.

Statistical Analysis

As part of this project, R. Colony developed statistical methods that use observed buoy drift and geostrophic wind data, to estimate the previous locations of ice found at the ULS site at any particular time. The method is being coded as a FORTRAN program that will enable us to better interpret the Greenland Sea ULS ice draft distributions in terms of their origin and trajectory.

Plans

We plan to continue our analysis of the ULS data, from two standpoints: (1) as instrument test data, and (2) as valuable new monitoring data on the ice thickness distribution. The analysis of remote sensing data will proceed, now that we have ice thickness data with which to compare it.

New Research

In the time period 1989-91 we propose two extensions of the ULS work:

(1) A modest engineering effort to enhance the ULS design as described previously.

(2) To build, test and deploy several new ULS units, in connection with the Greenland Sea Project and other initiatives, and as a contribution to the Arctic Ice Thickness Monitoring Program of the World Climate Research Program (WMO). This effort will be coordinated with other investigators interested in monitoring ice draft: K. Aagaard, E. Carmack, P. Lemke, T. Vinje, E. Augstein, and J. Meincke. The logistics plans once again take advantage of the numerous moorings of opporunity scheduled in 1989-1991. The prime scientific objective of this work is to obtain space and time coverage of ice thickness distribution sufficient to estimate accurately the ice mass balance of the Greenland Sea and the Arctic Ocean.

Publications

A data report from APL-ULS1 is attached. Two manuscripts are in preparation. One describes the new instrument and its performance. The second presents an analysis of the ice thickness data from the Chukchi Sea, together with ice motion and wind observations from the Arctic Buoy Program, and remote sensing imagery of the Chukchi Sea.

References

Bourke, R.H. and R.P. Garrett, Sea ice distribution in the Arctic Ocean, *Cold Reg. Sci. Tech.* 13, 259-280, 1987.

Bourke, R.H. and R.G. Paquette, Estimating the thickness of sea ice, *J. Geophys. Res.*, 94 (C1), 919-923, 1989.

Colony, R., A new look at sea ice thickness, 9th Int'l. Conf. Port Ocean Engr. Arctic (POAC-87), Fairbanks, 9 pp., 1987.

Feldman, H.R., P.H. Moose and S.R. Shah, Measurements of the volume scattering strength in the Beaufort and Chukchi Seas, Ocean '73, IEEE, New York, 508-513.

Francois, R.E., High resolution observations of under-ice morphology, APL-UW 7712, Applied Physics Lab, U. Washington, Seattle, 30 pp., 1977.

Francois, R.E. and G.R. Garrison, Sound Absorption ..., *J. Acoust. Soc. Am,* 72 (6), 1982.

Garrison, G.R., T. Wen and M.L. Welch, Environmental measurements in the Beaufort Sea, autumn, 1984, APL-UW 3-85, Applied Physics Lab, U. Washington, Seattle, 1985.

Garrison, G.R., T. Wen, R.E. Francois, W.J. Felton and M.L. Welch, Environmental measurements in teh Beaufort Sea, spring, 1986. APL-UW 4-86, Applied Physics Lab, U. Washington, Seattle, 59 pp, 1987.

Hunkins, K., The seasonal variation in the sound-scattering layer observed at Fletcher's Ice Island (T-3) with a 12 kc/s echosounder, *Deep Sea Res.,* 12, 879-881, 1965.

Johnsen, A.S., Upward Looking Sonar, do we get the mean ice thickness?, personal communication, 3 pp, 1989.

Parkinson, C.L., J.C. Comiso, H.J. Zwalley, D.J. Cavalieri, P. Gloersen, and W.J. Campbell, Arctic sea ice, 1973-1986: satellite passive microwave observations, NASA Sci. Tech. Info. Branch, Washington, D.C., 296 pp.

Rothrock, D.A., Ice thickness distribution - Measurement and theory, in: *The Geophysics of Sea Ice,* (N. Untersteiner, ed), Plenum Press, New York, 551-575, 1986.

Rothrock, D.A. and A.S. Thorndike, Geometric properties of the underside of sea ice, *J. Geophys. Res.,* 85 (C7), 3955-3963, 1980.

Thorndike, A.S., D.A. Rothrock, G.A. Maykut and R. Colony, The thickness distribution of sea ice, *J. Geophys. Res.,* 80 (33) 4501-4513.

Thorndike, A.S., Testing the thickness distribution theory, in: *Sea Ice Processes and Models* R. Pritchard (ed), Univ. of Washington Press, Seattle, 144-150, 1980.

Urick, R.J., *Principles of Underwater Sound for Engineers,* McGraw-Hill, 384 pp., 1975.

Vinje, T.E. and O. Finnekasa, The ice transport through Fram Strait, Norsk Polar Institutt Skrifter, NR. 186, Oslo, 39 pp, 1986.

Wadhams, P., Sea ice thickness distribution in Fram Strait, *Nature,* 30 (5930) 108-111, 1983.

Wadhams, P., *Nature,* 1990.

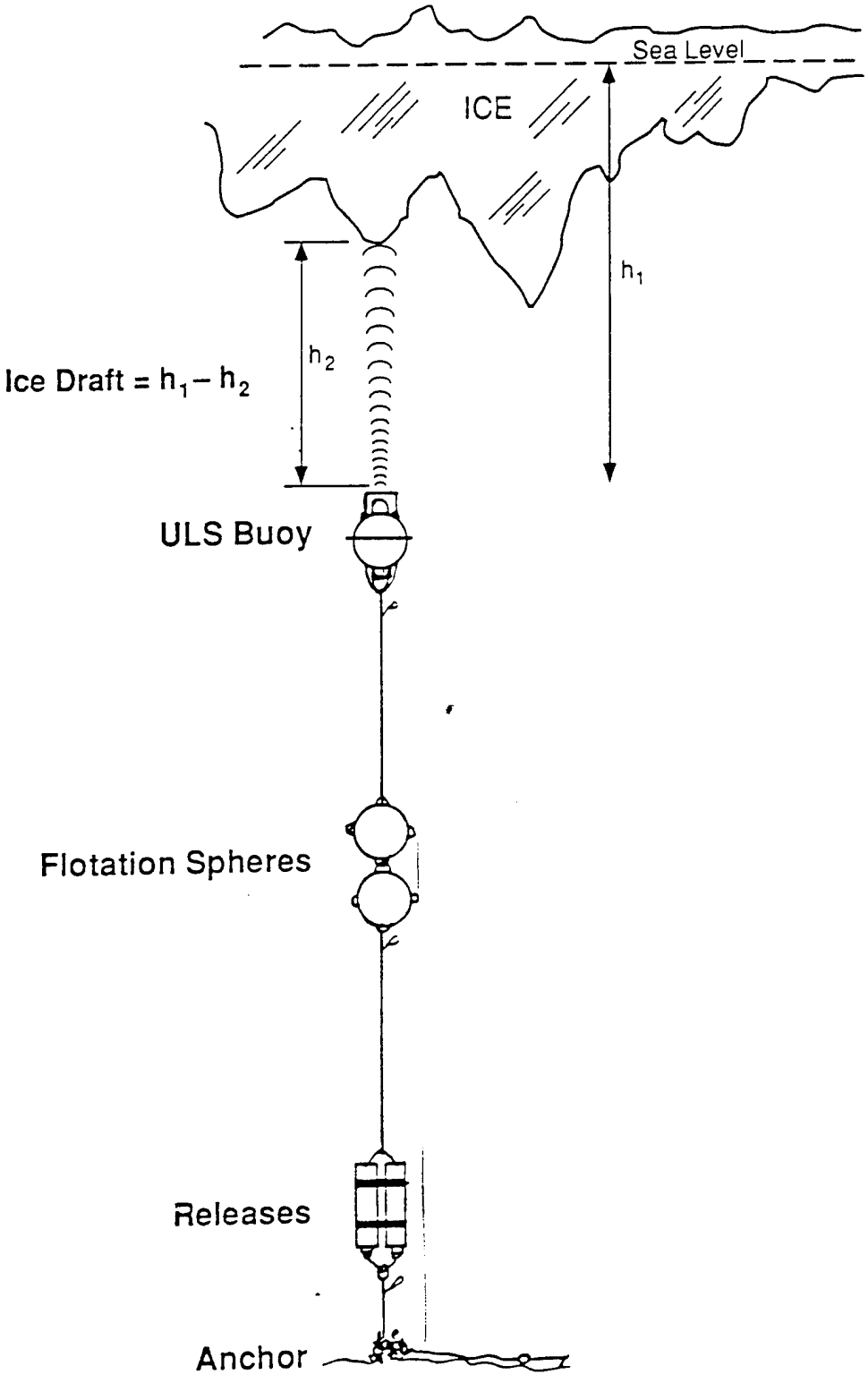

Figure 1: Operating configuration of the ULS. Depth below sea level h_1 measured by barometer, distance to ice h_2 measured by sonar. Ice draft h is $h_1 - h_2$.

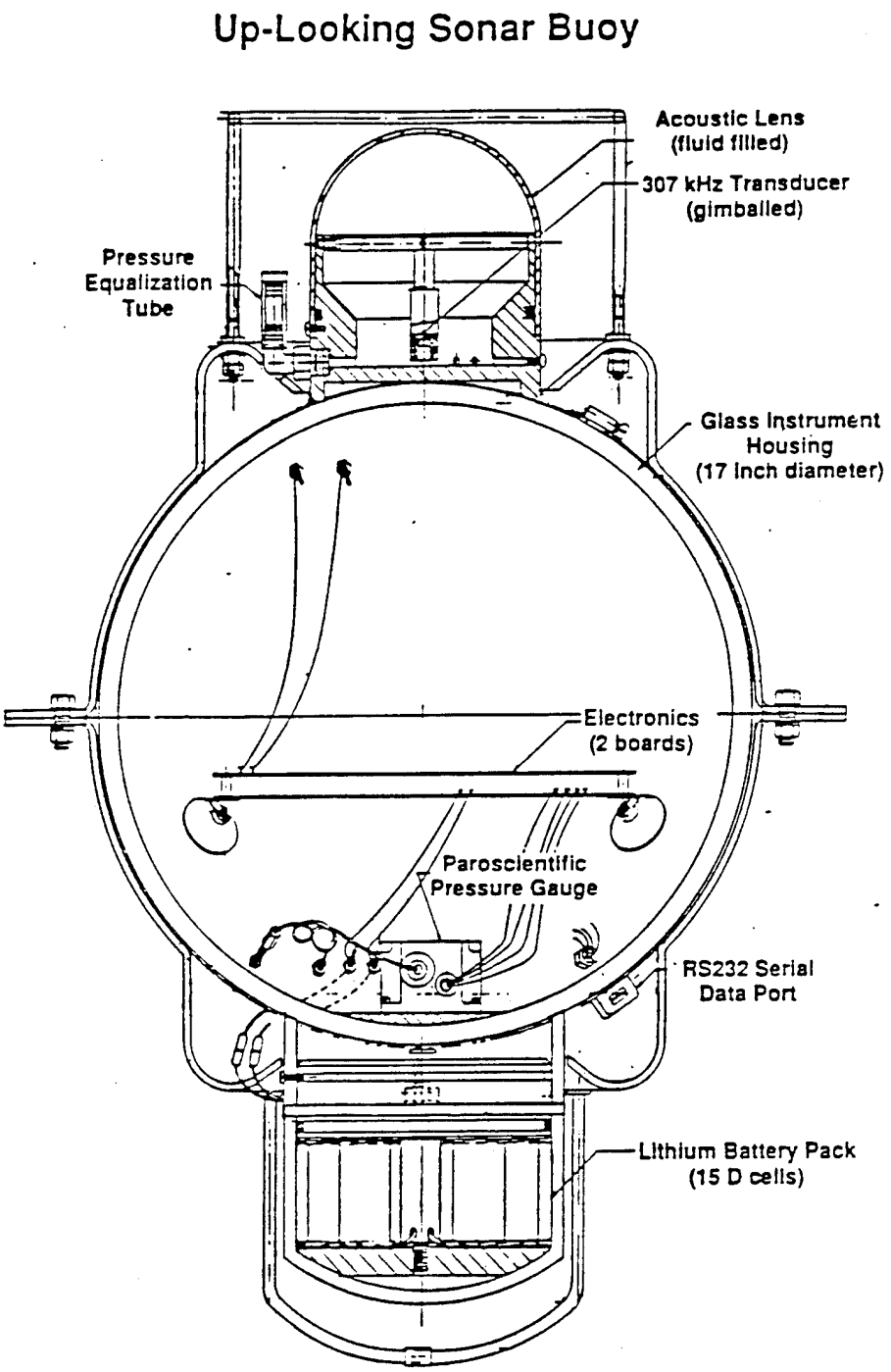

Figure 2: Schematic of the ULS Mark-1 instrument, illustrating the main components inside and outside the glass housing. The housing diameter is 17 inches.

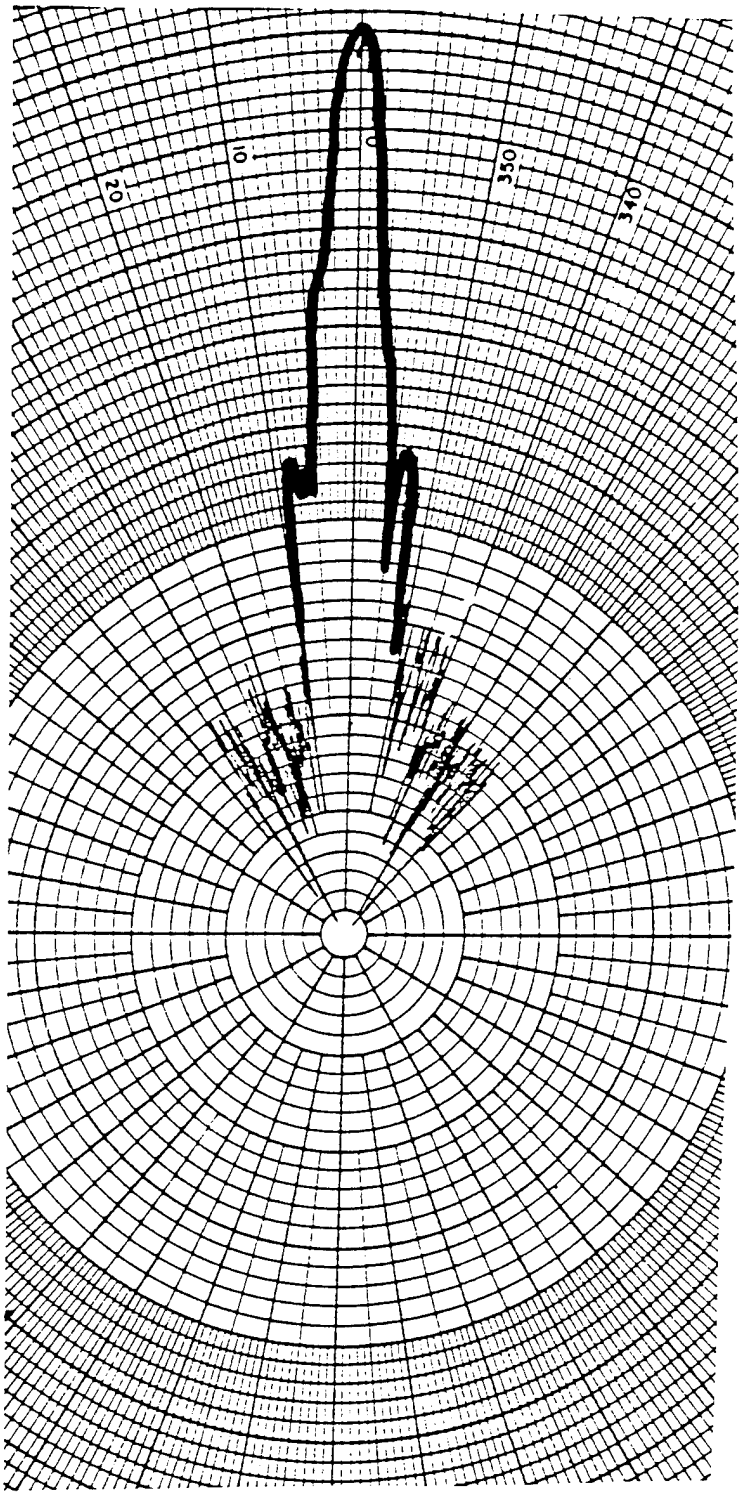

Figure 3: Transmit beam intensity pattern for a focused lens, ULS Mark-1. Response is measured radially (1 *dB* increments). Angular deviation from beam center is measured azimuthally (1^o increments). This pattern has a beamwidth $y \approx 1.3^o$.

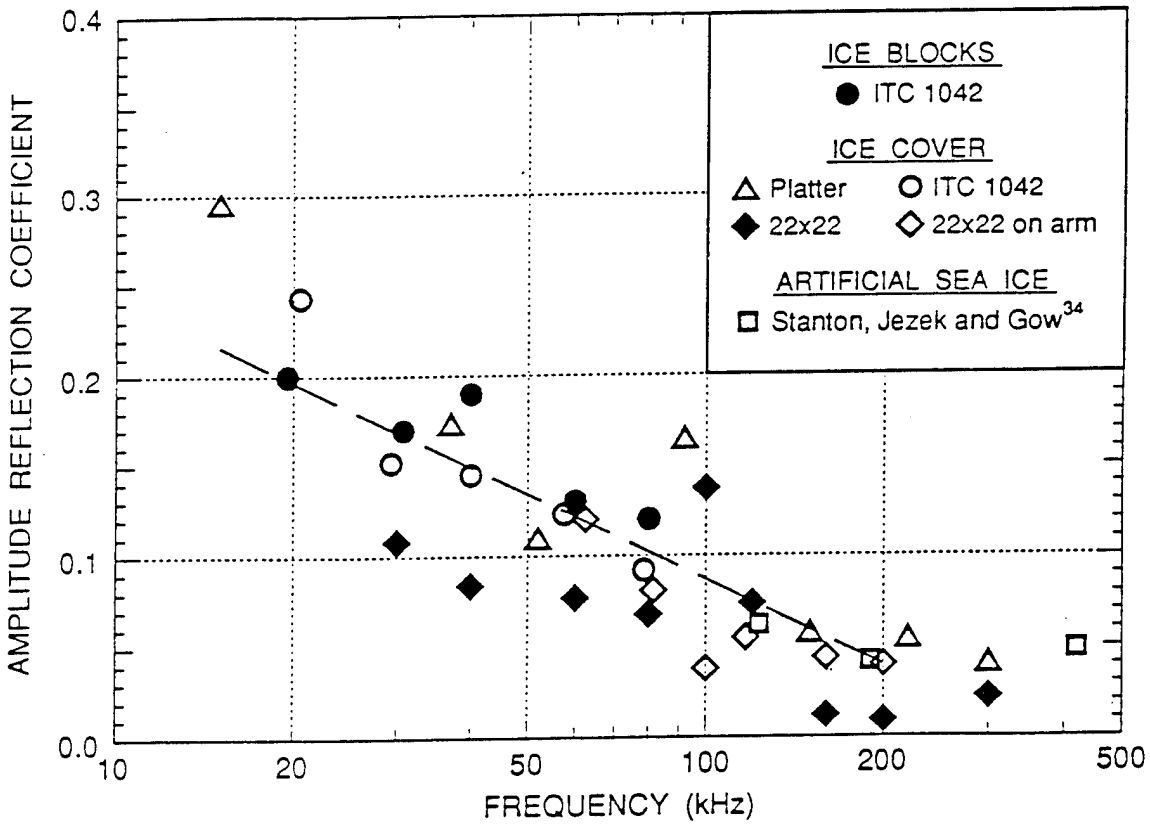

Figure 4: Effective amplitude reflection coefficient from level sea ice, for a range of acoustic frequencies. (from Francois, 19--).

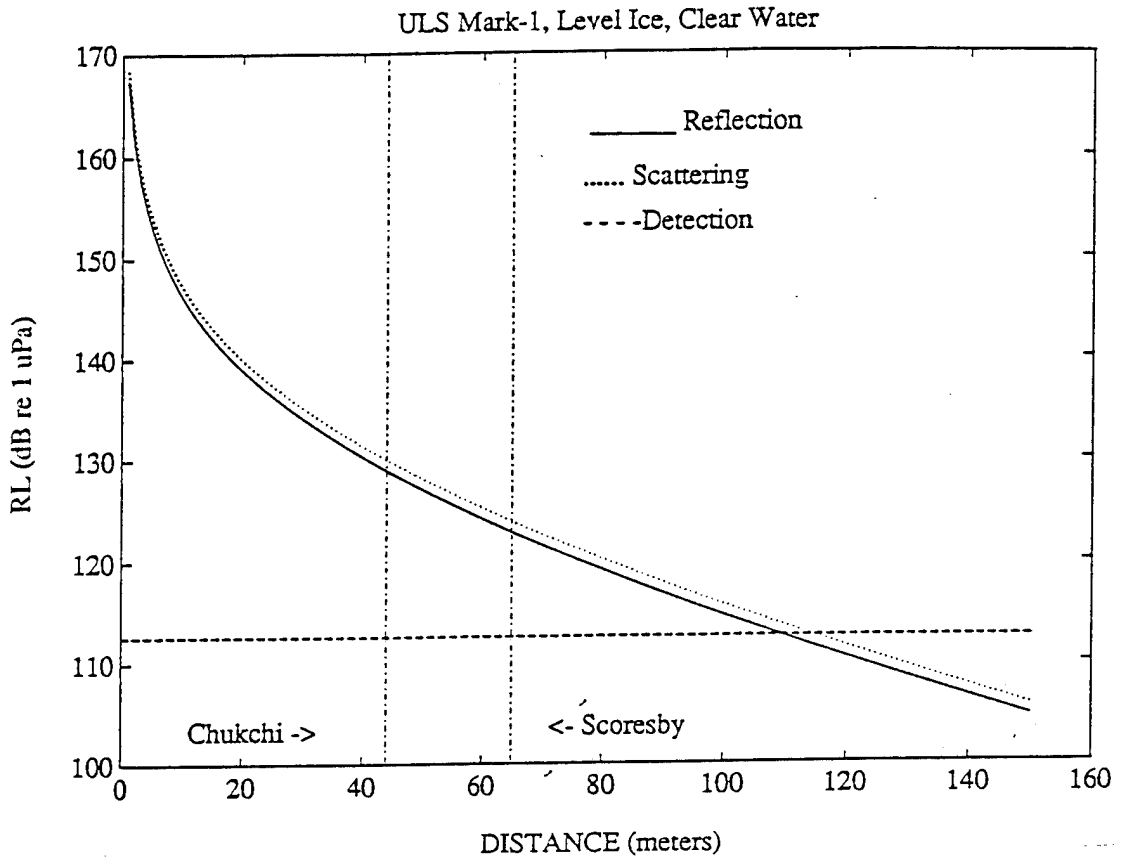

Figure 5: Received level as a function of distance for ULS Mark-1, level ice target with zero volume reverberation.

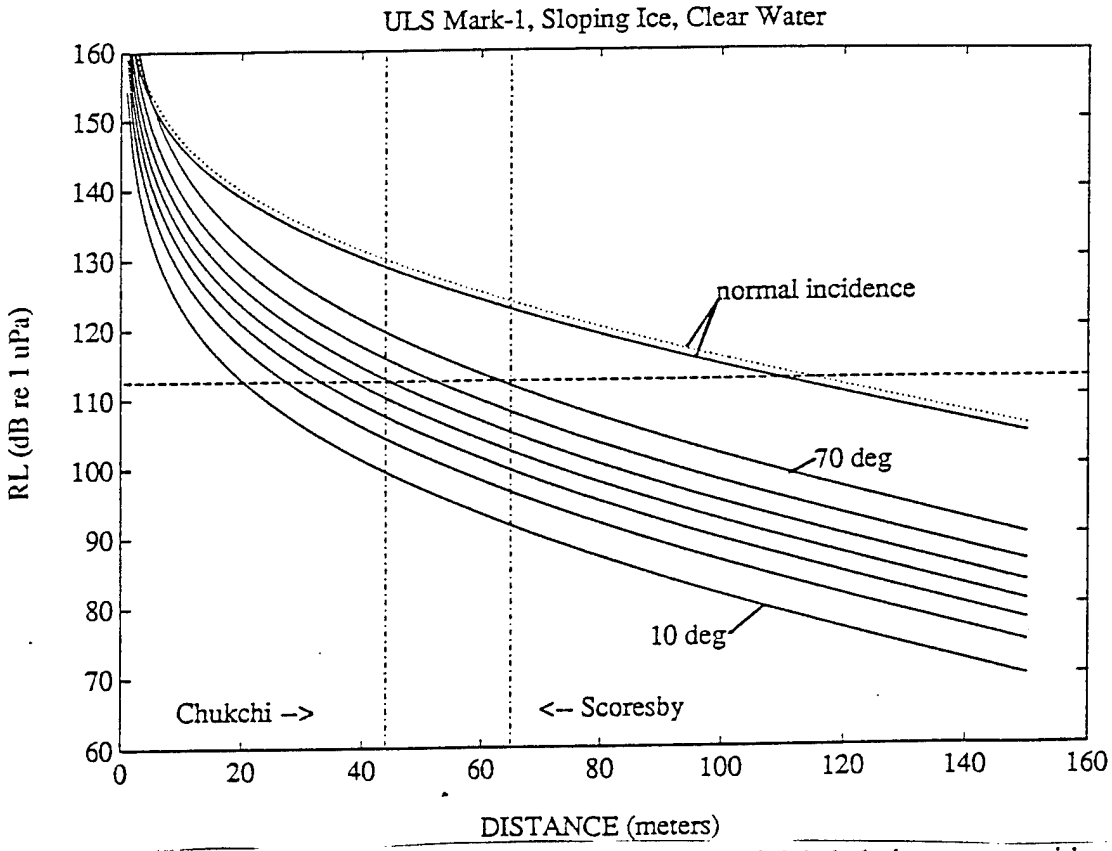

Figure 6: Received level as a function of distance for ULS Mark-1, ice targets with grazing angles at 10^o intervals from $10^o - 70^o$. Level ice curves from Figure 5 are shown for comparison.

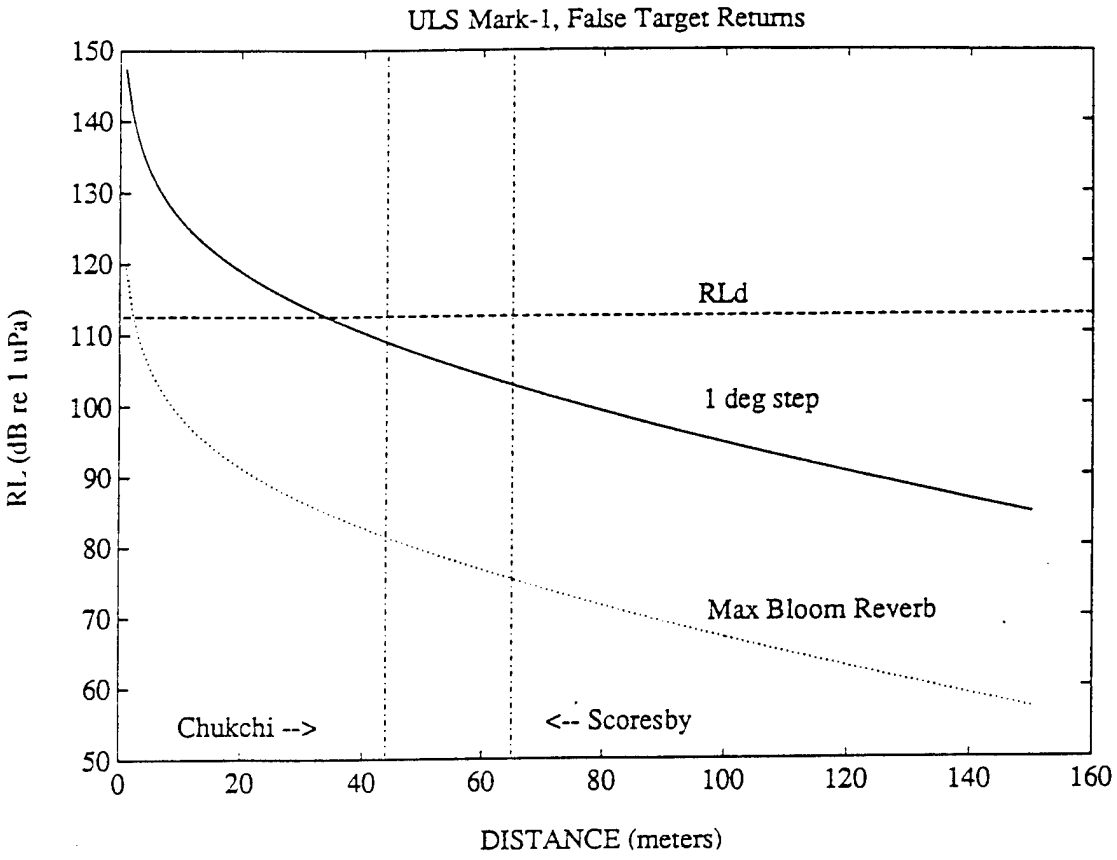

Figure 7: Received level as a function of distance for ULS Mark-1. Targets are: 1^o *C* temperature step in seawater (solid curve) and volume reverberation from maximal plankton bloom (dotted curve).

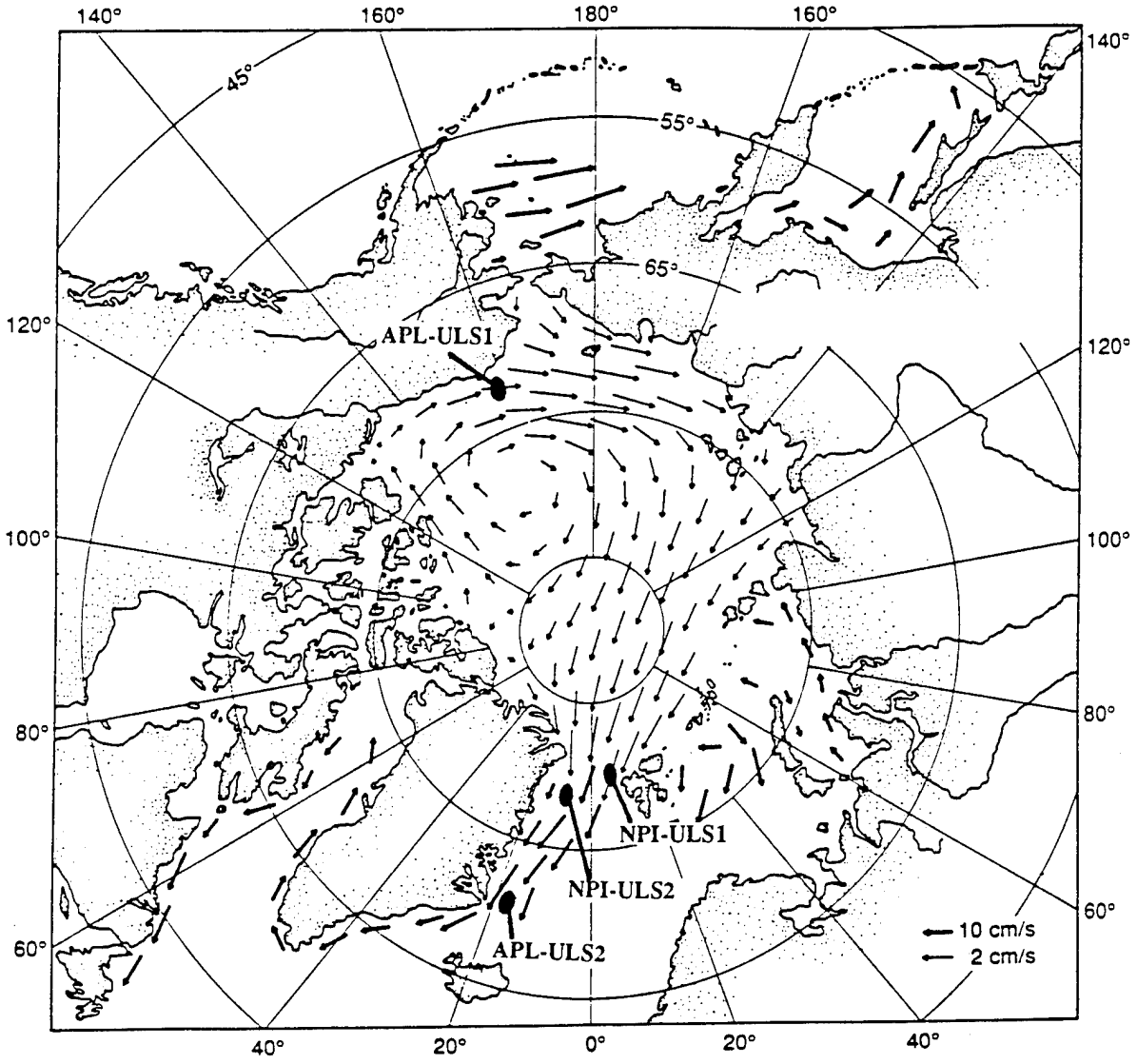

Figure 8: Locations of ULS Mark-1 deployments in 1988. Instruments denoted "NPI" were purchased and deployed by the Norsk Polar Institutt.